Circuits and Systems, 2013, 4, 58-66
http://dx.doi.org/10.4236/cs.2013.41010 Published Online January 2013 (http://www.scirp.org/journal/cs)

A Current Bleeding CMOS Mixer Featuring *LO* Amplification Based on Current-Reused Topology*

Wah Ching Lee [1,2], Kim Fung Tsang[2], Yi Shen[2], Kwok Tai Chui[2]
[1]Department of Electronic & Information Engineering, The Hong Kong Polytechnic University, Hong Kong, China
[2]Department of Electronic Engineering, City University of Hong Kong, Hong Kong, China
Email: enwclee@inet.polyu.edu.hk, ee330015@cityu.edu.hk, yishen@cityu.edu.hk, ktchui3@student.cityu.edu.hk

Received August 30, 2012; revised September 30, 2012; accepted October 8, 2012

ABSTRACT

A double balanced Gilbert-cell class-A amplifier bleeding mixer (DBGC CAAB mixer) is proposed and implemented. The injection current is utilized to amplify the local oscillator (*LO*) signal to improve the performance of the transconductor stage. The DBGC CAAB mixer achieves a conversion gain of 17.5 dB at −14 dBm *LO* power, and the noise figure is suppressed from 45 dB to 10.7 dB. It is important to stress that the new configuration will not drain additional power in contrast to the former current bleeding mixers. This topology dramatically relieves the requirement of the *LO* power. The DBGC CAAB mixer is implemented by using 0.18-μm RFCMOS technology and operates at the 2.4 GHz ISM application with 10 MHz intermediate frequency. The power consumption is 12 mA at 1.5 V supply voltage. The DBGC CAAB mixer features the highest FOM figure within a wide range of *LO* power.

Keywords: Mixer; Gilbert-Cell; Current Bleeding; Noise; Conversion Gain; Current-Reuse; Class-A Amplifier

1. Introduction

With the rapid proliferation of modern wireless market, RF transceivers play a more and more important role in our daily lives. Mixer is one of the key blocks in the signal chain performing frequency translation before signals are further processed in the intermediate frequency circuits. The noise and the gain performance of the mixer, in general, determine the performance of the whole system at large [1]. In past decades, many research scholars made deep insights into the noise mechanism [2-5] and gain enhancement [6-8] in mixers. In order to achieve good performance including gain, noise, isolation and linearity (higher-order components), Gilbert-cell [9] is commonly used as the mixer core topology.

Amongst most factors, the conversion gain (CG) and the third-order intercept point (IP3) of the mixer are the key elements determining the mixer performance. Both CG and IP3 are proportional to the square root of the bias current (I_{b1}) of the driver stage [10,11], as shown in **Figure 1(a)**. In order to improve CG and IP3, a simple method is to increase the bias current of the driver stage M1, namely I_{b1}. However, this improvement is at the expense of other degradations. For instance, the increase of I_{b1} will also increase the currents, I_{b2} and I_{b3}, in the switch pair M2 and M3 (referred as M2-M3 thereafter). As a result, the noise contributions from M2-M3 are also increased [12-14]. In addition, in order to keep all the transistors working in saturation region, the load resistance Z_L should be decreased to avoid too much voltage drop across them, especially in modern sub-micro CMOS technology. The load resistance reduction will in turn cause the gain compression. Hence it is concluded that increasing the bias current solely of the driver stage is not an efficient way to improve the overall performance, including gain, linearity and noise of the mixer.

In order to retain the benefits of increasing the bias current but without degrading other performances, a current bleeding topology, by applying a current source in

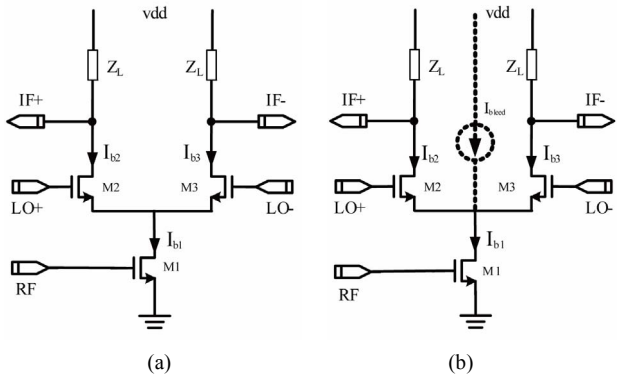

Figure 1. Schematic of (a) Conventional single-balanced mixer; (b) Single-balanced mixer with current bleeding.

*The work was supported by Research Grants 9220049 from City University of Hong Kong.

parallel with M2-M3, is used [15]. Analysis shows that such topology [15], [16] facilitates the quiescent current in the driver stage to be independent from M2-M3. **Figure 1(b)** shows the illustrative topology. The bleeding current source drives a higher driver stage current through the higher load resistance of M1 by virtue of the fact that part of the driver bias current is steered from M2-M3. An additional advantage of using the bleeding source is that M2-M3 can operate at a lower gate-source voltage and thus rendering a compact size. Lower gate-source voltage helps to improve the conversion efficiency as fewer charges are necessary to turn M2-M3 on and/or off.

In this paper, a double balanced Gilbert-cell class-A amplifier bleeding mixer (DBGC CAAB mixer) is developed. By inserting a class-A amplifier in parallel with M2-M3, the local oscillator (*LO*) swing is increased to drive M2-M3 into a hard switching fashion. An additional advantage is that the bias current of the class-A amplifier will enhance the bias of the driver stage of the mixer, hence improving the overall performance. The present investigation is an extension of our previous work [17] with a detailed analysis of noise reduction and gain boosting. Detailed measurement results are also provided. The paper is organized as follows: Section 2 describes the motivation of this work; Section 3 describes the topology, the design and the analysis results, Section 4 summarizes the performance of the developed mixer by including a FOM comparison and, Section 5 gives the conclusion.

2. Motivation

In the mixer analysis, the drain current of M2-M3 are presented as:

$$I_{D2} = K\left(V_{GS2} - V_T\right)^2 \tag{1}$$

$$I_{D3} = K\left(V_{GS3} - V_T\right)^2 \tag{2}$$

The voltage of Local Oscillator (*LO*), v_{LO}, is defined as:

$$v_{LO} = V_{GS2} - V_{GS3} \tag{3}$$

From KCL:

$$I_{D1} = I_{D2} + I_{D3} \tag{4}$$

and, for the differential operation of M2-M3, the output current is:

$$I_{\text{out}} = I_{D2} - I_{D3} \tag{5}$$

Based on the physics of the MOS device, Equations (1) and (2) are supported by the following relationships:

$$K = \frac{1}{2}\mu_n C_{ox}\frac{W}{L} = \frac{I_{D1}}{2V_{od}^2} \tag{6}$$

$$V_{od} = V_{GS} - V_T \tag{7}$$

In order to characterize the relationship of the output current and the performance of M2-M3, the output current is derived as a function of v_{LO}:

$$I_{\text{out}} = Kv_{LO}\cdot\sqrt{\frac{2I_{D1}}{K} - v_{LO}^2} \tag{8}$$

This formula is derived based on the condition that both M2 and M3 are at ON state. When $v_{LO} > \sqrt{2}V_{od}$, M2-M3 acts as a hard switch, and the output current, I_{out}, can be modeled as a sgn function:

$$I_{\text{out}} \approx \begin{cases} I_{D1}\cdot\sqrt{1-\left(1-\delta^2/2\right)^2}, |\delta| \le \sqrt{2} \\ I_{D1}\cdot\text{sgn}\left(\delta\right), |\delta| \gg \sqrt{2} \end{cases} \tag{9}$$

where, $\delta = v_{LO}/V_{od}$

Figure 2 shows the I-V characteristics of M2-M3 graphically. The transconductance of M2-M3, G_m, is given by:

$$G_m\left(v_{LO}\right) = 2\frac{g_{m2}\left(v_{LO}\right)\cdot g_{m3}\left(v_{LO}\right)}{g_{m2}\left(v_{LO}\right) + g_{m3}\left(v_{LO}\right)} \tag{10}$$

It will be explained in (13) that increasing v_{LO} will improve the mixer performance; hence the dependence of G_m on v_{LO} needs to be investigated. G_m is derived as a function of v_{LO}:

$$G_m\left(v_{LO}\right) = 2I_{D1}\sqrt{\frac{1}{v_{LO}^2 + \frac{2I_{D1}}{K}}} \tag{11}$$

As shown in **Figure 2**, $G_m\left(v_{LO}\right)$ reaches its maximum value as v_{LO} approaches 0. When v_{LO} increases, $G_m\left(v_{LO}\right)$ decreases and eventually approaches zero.

Noise is an important parameter in mixer design and is now discussed. In general, there are three main noise

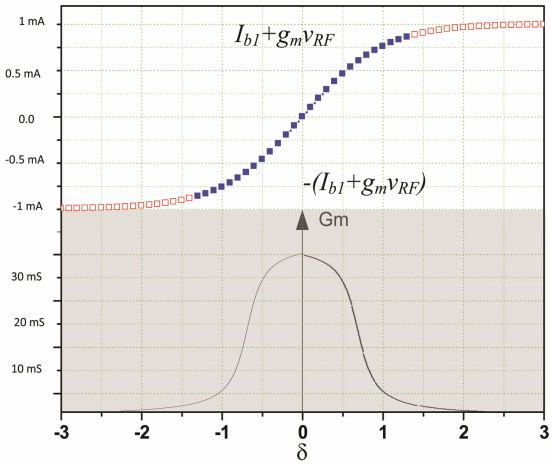

Figure 2. I-V characteristic and equivalent transconductance of M2-M3, where $\delta = v_{LO}/V_{od}$.

sources in conventional mixer circuits, namely the trans-conductor stage, the switch pair M2-M3 and the load. In Terrovitis [5] and Darabi [2] models, noise contributed to the output exactly when both switching transistors are at ON state—indicated as the switch interval Δ (will be discussed in Section 3). The noise PSD (power spectrum density), introduced within Δ is presented as:

$$PSD = 8KT\gamma G_m = 16KT\gamma\left(\frac{g_{m2}\cdot g_{m3}}{g_{m2}+g_{m3}}\right) \quad (12)$$

where K—*Boltzmann's constant*

T—*Absolute temperature*

γ—*noise coefficient* (= 2/3 *for long channel device*)

g_{m2}, g_{m3}—*Trans-conductance of* M2-M3

At the zero-crossing point of v_{LO}, both M2 and M3 are at ON state, thus resulting in non-zero value of g_{m2} and g_{m3}. From (11), large *LO* voltage swing will diminish G_m, rendering either g_{m2} or g_{m3} to vanish and thus suppressing the noise. Noise PSD can further be converted [5] to the relationship of bias current and noise contribution:

$$PSD = \frac{16KT\gamma}{\pi}\cdot\frac{I_B}{v_{LO}} \quad (13)$$

where I_B is the bias current of M2-M3. It is seen from (13) that, by increasing v_{LO}, Noise PSD is suppressed efficiently. Furthermore, by reducing I_B, PSD will also be suppressed, thus further verifying the current bleeding principle.

The other key parameter of a mixer is gain. In order to enhance the gain, the conversion gain (CG) of the mixer is also analyzed [5].

$$CG = c\cdot g_{m1}\cdot re\{Z_L\} \quad (14)$$

where the multiplier c is given by:

$$c \approx \frac{2}{\pi}\left(\frac{\sin(\pi\Delta/T_{LO})}{\pi\Delta/T_{LO}}\right) \quad (15)$$

It is seen from (15) that increasing c, and/or g_{m1}, is an efficient way to increase CG. The implementation will be discussed in Section 3.4.

Based on the above discussion, the novelties of the proposed design are:

A1) Novel bleeding source: In order to improve the gain, linearity and noise, the bias current of the driver stage should be increased. However, such a direct increase will cause other related problems, including the high noise contribution from M2-M3 as well as the excessive voltage drop on the load resistor. It is important to note that the current bleeding structure improves only the bias of the driver stage but without increasing the bias of M2-M3.

A2) *LO* amplification: Higher amplitude of V_{LO} helps to minimize the noise PSD from the M2-M3 by reducing Δ, and at the same time, maximizing $CG\left(=2\cdot(g_{m1})\cdot(Z_L)/\pi\right)$ to reach the upper limit.

In this investigation, a Gilbert-cell mixer based on the current bleeding technique is explored. Inspired from the benefit of high gain and low noise (referring to (A1) and (A2)), and taking advantage of the linearity, a class-A amplifier (referred as **Amp** thereafter), is implemented as the bleeding sources to amplify the *LO* signals. Hence the class-A amplifier bleeding source is employed to replace the traditional simple current source. After performing the *LO* amplification, the DC bias current of the class-A amplifier is steered to the driver stage of the mixer to improve the gain, noise and linearity characteristics. It will be explained that, comparing to the conventional current bleeding mixer, the CAAB structure can reuse the bleeding current more efficiently.

3. Methodology

3.1. Overall Topology

Figure 3 shows the proposed double-balanced Gilbert-cell mixer incorporating CAAB, namely DBGC CAAB mixer. As shown in **Figure 1(b)**, taking advantage of the symmetry, one half of the circuit is used for analysis. In conventional mixers, the bias current, I_{b1}, of the driver stage M1 is the sum of current of I_{b2} (of M2) and I_{b3} (of M3), *i.e.* $I_{b1} = I_{b2} + I_{b3}$. However, in a DBGC CAAB mixer, the bias current of M1 is the sum of I_{b2}, I_{b3} and I_a, *i.e.* $I_{b1} = I_{b2} + I_{b3} + I_a$. By devising component values for **Amp**, V_{LO} of M2-M3 is increased, thus reducing Δ, and rendering a noise reduction in M2-M3.

3.2. The Amp Design

The **Amp** in **Figure 3** is implemented as shown in **Figure 4**. As described in the preceding section, the bias current I_a is steered into the driver stage M1 of the mixer. Thus the provision of a uniform current (I_a) is crucial to the performance of the mixer since any potential large

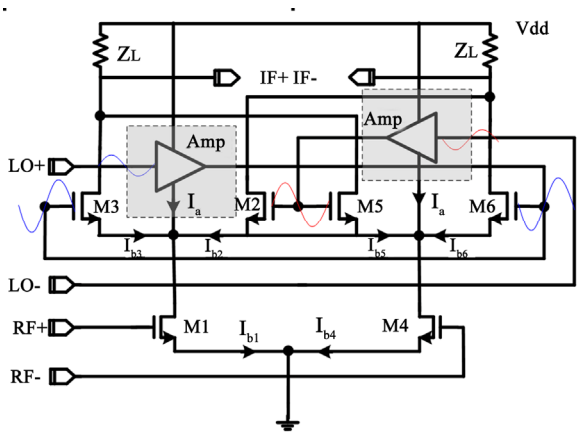

Figure 3. Schematic of DBGC CAAB mixer.

disturbance of I_a may cause gain ripples and non-linear degradations in the driver stage M1. In this case, since 0.18-μm fabrication process is used, the channel length of the transistor is small, rendering I_a more and more susceptible to the channel length modulation [18]:

$$I_a = \frac{1}{2}\mu_n C_{ox}\frac{W}{L}\left(V_{GS}-V_{TH}\right)^2\left(1+\lambda V_{DS}\right) \quad (16)$$

The large output voltage swing normally appearing on the drain of the transistor will change the V_{DS} dramatically and periodically. In principle, in order to avoid the channel length modulation, a cascode topology can be employed. However, this structure will limit the output voltage swing. An alternative method is to use a longer channel length. In this investigation, 0.35-μm gate length is preferred as the operating frequency is not very high (2.5 GHz).

It is important to stress that, in order to lower the inherent noise in the CAAB mixer, the **Amp** is realized as a low noise amplifier. In **Figure 4**, the components L_g, C_{gs}, C_{sr}, L_{sr} and L_s are used for noise matching [19]. In order to further analyze the amplifier, the equivalent circuit is shown in **Figure 5**. By using a large value of L_s (for isolating RF signals and *LO* signals), the impedance Z_m can be considered as open. C_{sr} is a relatively large value capacitor used for blocking the DC current but will not influence significantly on the series combination of C_{gs} and C_{sr}:

$$\frac{1}{C_{comb}} = \frac{1}{C_{gs}} + \frac{1}{C_{sr}}$$

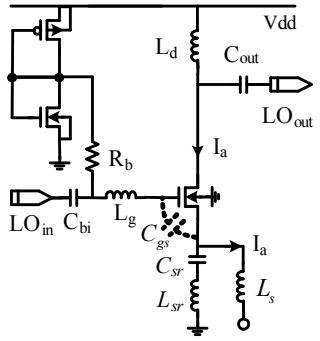

Figure 4. Topology of current bleeding source—Amp (class-A amplifier).

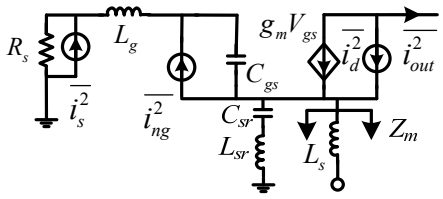

Figure 5. Equivalent circuits of the class-A amplifier (Amp) in Figure 4.

The input impedance Z_{in} is then degenerated to be:

$$Z_{in} \approx s\left(L_g + L_{sr}\right) + \frac{1}{sC_{comb}} + \frac{g_m}{C_{gs}}L_{sr} \quad (17)$$

At resonance, the imaginary part of Z_{in} vanishes, and the real part is left for 50 Ω matching [19]. The **Amp** operates at a DC bias current of 4.5 mA.

3.3. The DBGC CAAB Mixer and Implementation

The **Amp** is then designed and analyzed by SpectreRF in Cadence. Compromising the power consumption, *LO* amplification and stability, the gain of the **Amp** to be designed is chosen to be about 14 dB. The component values in **Figure 5** are optimized as:

$L_g = 8.5$ nH, $C_{gs} = 0.7$ pF, $C_{sr} = 20$ pF, $L_{sr} = 1.2$ nH.

Figure 6 shows the final characteristics of **Amp**. **Figure 7** shows the voltage waveforms at the input and the output of the **Amp** at various *LO* input power levels. An investigation of the voltage waveforms reveals that the amplitude of the *LO* signal is amplified by a factor of five (5). The achieved input 1 dB compression point ($P_{1dB,in}$) is 3 dBm, thus surpassing the traditional performance that $P_{1dB,in} < 0$ dBm.

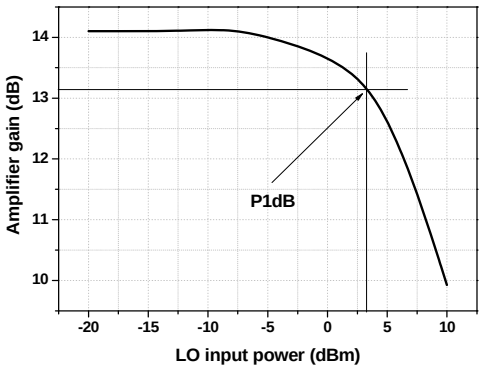

Figure 6. The simulated voltage gain of the Amp.

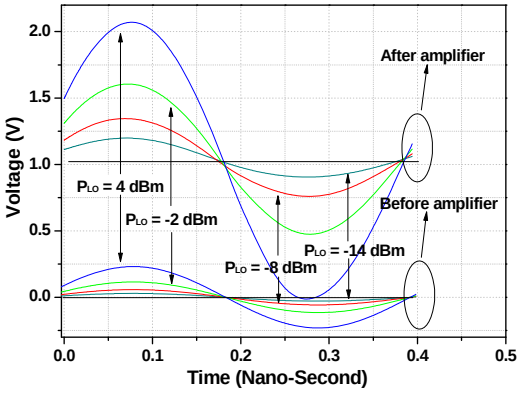

Figure 7. The voltage swing at the input and the output of Amp at varying input power level.

The DBGC CAAB mixer is realized by a 0.18-μm 1-poly 6-metal RFCMOS technology. A microphotograph of the device is shown in **Figure 8**. The chip occupies an area of 1.2 × 1.3 mm^2. Under nominal operation, the mixer extracts 12 mA from the 1.5 V supply. The chip was bonded to a FR4-PCB board with gold-wire for measurement. The operating frequency is 2.4 GHz with 10 MHz IF as the output frequency for testing purpose.

3.4. Noise Analysis

In essence, the *LO* signal is a sinusoid rather than a square wave, rendering that the current switching to approximate a soft-switch with switch interval Δ (see **Figure 9**). When $v_{LO} < V_X$, (V_X is the threshold voltage of M2-M3) both transistors of M2-M3 are "ON", and the current division ratio is biased dependently such that the total bias current of M2-M3 is constant: when M2 is biased in high level, the current flow through M2 increases, and the current in M3 decreases. When $v_{LO} > V_X$, the current will flow through one of the transistors and the other counterpart is turned off. At this point, the "ON" transistor acts as the cascode stage of the driver stage.

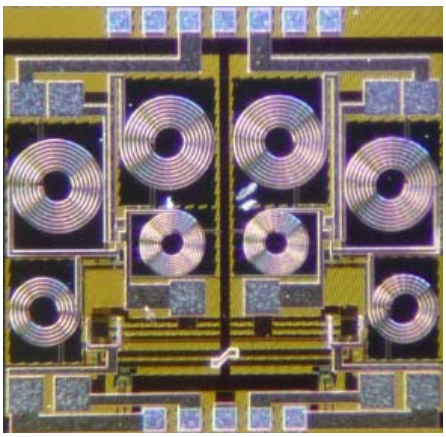

Figure 8. Microphotograph of the implemented DBGC CAAB mixer.

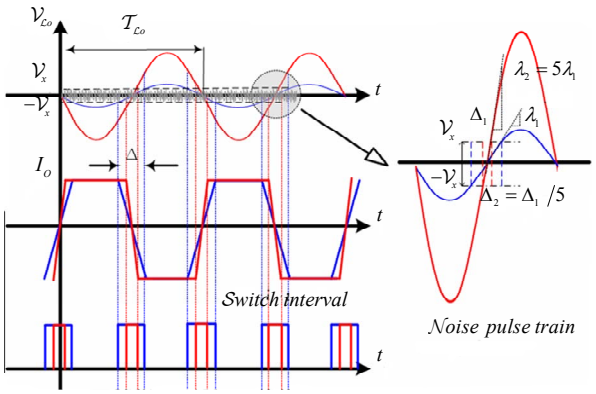

Figure 9. The influence of v_{LO} on Δ and the resulting noise contribution.

The output noise component from M2-M3 is dictated by the relationship in (10) and (12), in which g_{m2} and g_{m3} are time-varying transconductances of M2-M3 under large *LO* drive. When $v_{LO} > V_X$, either M2 or M3 is cutoff and g_m vanishes. Consequently, G_m, as well as *PSD*, also vanish. When $v_{LO} < V_X$, the non-zero G_m proliferates M2-M3 to contribute noise to the output.

Let $PSD = S_{sw,\text{within}}$ when $v_{LO} < V_X$ and $PSD = S_{sw,\text{outside}}$ when $v_{LO} > V_X$. For analysis purpose, $S_{sw,\text{within}}$ is normalized to a train of pulses [4] operating at a rate $2f_{LO}$, as shown in **Figure 9**. The width of Δ is V_X/λ, where λ is the slope of *LO* waveform at the zero-crossing point, and is given by:

$$\lambda = 2\pi v_{LO}/T_{LO} \tag{18}$$

It was illustrated in Section 3.4 that by devising the **Amp**, v_{LO} has been amplified by five (5) times, thus the switch interval Δ_2 (after amplification) has been compressed to one fifth of Δ_1 (before amplification) (see **Figure 9**).

To further analyze the relationship between the noise PSD and the slope of *LO* waveform, λ, at the zero-crossing point, (12) is modified and derived as follows:

$$PSD = 32KT\gamma\frac{I_B}{\lambda T_{LO}} \tag{19}$$

From (19), it is analyzed and concluded that the noise from M2-M3 is reduced by a factor of five (5). Hence it is analyzed that:

$$V_{LO}\uparrow \Rightarrow \Delta\downarrow \Rightarrow \lambda\uparrow \Rightarrow S_{sw}(f)\downarrow$$

Additional noise improvement comes from the increasing bias of the driver stage due to the current bleeding source (here, it is DC bias of the **Amp**). Based on the original 1.5 mA DC bias current, the current bleeding source feeds additional 4.5 mA DC current to the driver stage. From [18], $g_{m1} = 2I_{B1}/(V_{gs} - V_{th})$, consequently, g_{m1} is improved by a factor of $\sqrt{4}$. For double-balanced mixer, the single-side band noise figure, NF [5], is rearranged as:

$$NF = \frac{\alpha}{c^2} + \frac{2r_{g1}\alpha + \dfrac{2\gamma_1\alpha}{g_{m1}} + \dfrac{4\gamma_3\bar{G} + 4r_{g3}\overline{G^2} + \dfrac{1}{R_L}}{g_{m1}^2}}{c^2 R_s} \tag{20}$$

where γ_1 and γ_3 represent the noise coefficient of M1 and M3 respectively. The poly resistance of the gate is indicated as r_{g1} and r_{g3}. It is seen from (20) that *NF* is inversely proportional to g_{m1}. Thus it is seen that the current bleeding improves g_{m1} dramatically and consequently suppresses the noise figure efficiently.

To examine the performance improvement of the DGBC CAAB mixer, an identical conventional Gilbert-quad mixer, without current bleeding—**Amp**, but having

the same transistor size in both the driver stage and the switch stage, is also designed with same process. Both mixers operate at 2.4 GHz input frequency with 10 MHz IF output. **Figure 10** shows the noise comparison at *LO* power from −20 dBm to 10 dBm. It is observed that the conventional mixer presents a noise figure in the range of 13 dB to 46 dB whereas the CAAB mixer features a much lower noise figure, namely from 9 dB to 11.5 dB. The inset of **Figure 10(b)** shows the measured noise figures versus *LO* power at 10 MHz intermediate frequency. The measured *NF* varies from 12.4 dB to 8.7 dB when the *LO* power is varied from −20 dBm to 10 dBm.

3.5. Conversion Gain Analysis

In the CAAB mixer, the conversion gain is affected by the switch stage M2-M3 and the driver stage. Recapitulated from (14), a Δdecreases, $\sin(\pi\Delta/T_{LO})/\pi\Delta/T_{LO}$ approaches to unit. As a result, the CG increases until reaching the upper limit $(2/\pi)\cdot g_{m1}\cdot R_L$. **Figure 11** illustrates the switch loss, L_{sw}, versus Δ. **Figure 11(a)** shows $L_{sw,\text{lin}}$, versus Δ due to the non-ideal square wave *LO* drive. **Figure 11(b)** intuitively shows the trend of $L_{sw,\text{dB}}$ (in logarithm scale) due to soft switching. **Table 1** lists the reduction of $L_{sw,\text{lin}}$ due to the *LO* amplitude amplification at four different Δ/T_{LO} cases. In the extreme case that Δ = 0.45 (when *LO* voltage is very weak), the gain improvement can be as high as 3 dB. It is also seen that when Δ is one fourth of the *LO* period (T_{LO}), which is the most probably case, $L_{sw,\text{lin}}$ can be improved from $0.9\cdot(2/\pi)\cdot g_{m1}\cdot R_L$ to $0.996\cdot(2/\pi)\cdot g_{m1}\cdot R_L$. As a result, 0.88 dB CG is gained.

It is shown in Section 2 that g_{m1} is improved by a factor of 4, hence an additional 12 dB gain is obtained. Thus, it is concluded that the current bleeding structure will boost g_{m1}, provoking a higher CG.

To examine the gain performance of the DBGC CAAB mixer, a comparison with the conventional mixer and other published works is shown in **Figure 12**. For the conventional mixer, the maximum gain achieved is 11 dB when *LO* port is fed by 10 dBm signal. In contrast, a gain of 17.5 dB is achieved when −14 dBm is fed to the *LO* port of the DBGC CAAB mixer. Thus, it is con-

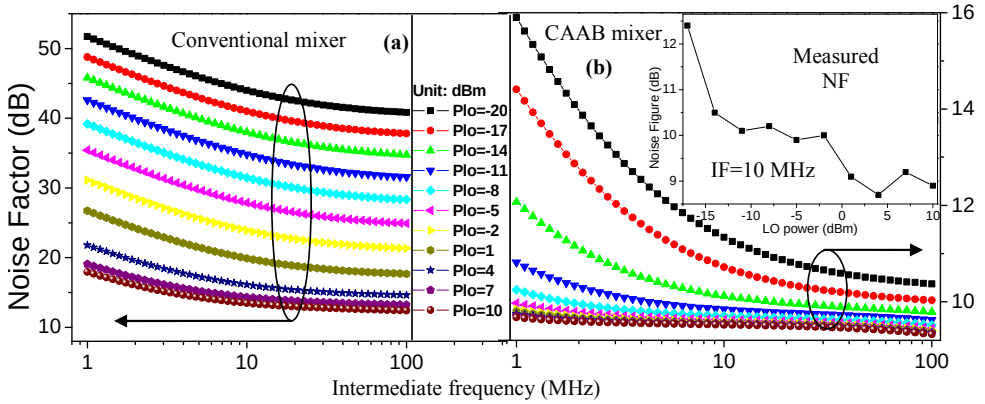

Figure 10. Noise figures at different *LO* input power. (a) Conventional mixer; (b) DBGC CAAB mixer; inset: measured *NF* at IF = 10 MHz.

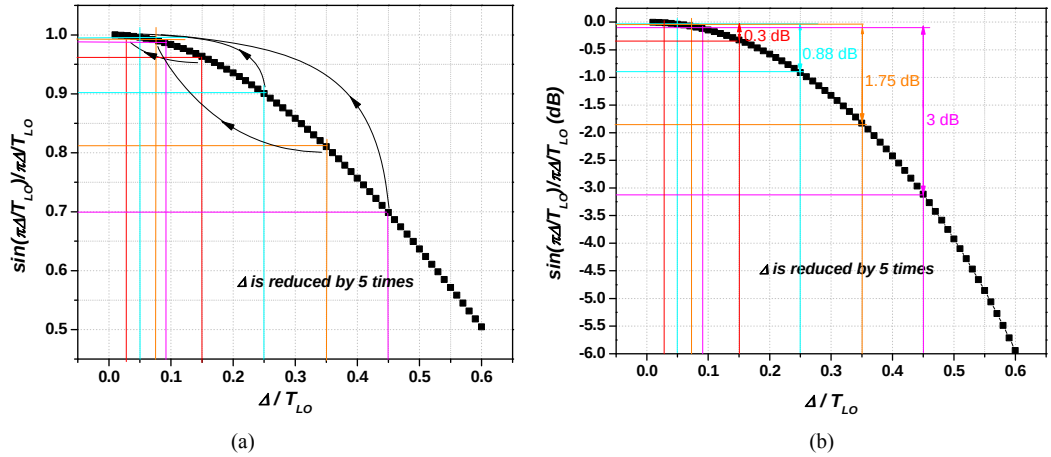

(a) (b)

Figure 11. The switch loss reduction due to the switch interval Δ shrinkage: (a) Linear scale; (b) Logarithm scale.

Table 1. The quantized switching loss reduction due to the *LO* amplification in linear and logarithm scale.

	$\sin(\pi\Delta/T_{LO})/\pi\Delta/T_{LO}$		$20\log\left(\frac{\sin(\pi\Delta/T_{LO})}{\pi\Delta/T_{LO}}\right)$		$20\log\left(\frac{\sin(\pi\Delta/T_{LO})}{\pi\Delta/T_{LO}}\right)$
	Linear scale		Logarithm scale (dB)		Logarithm (dB)
Δ/T_{LO}	Without **Amp**	With **Amp**	Without **Amp**	With **Amp**	Switching loss reduction
0.15	0.9634	0.99852	−0.3239	−0.01286	0.3
0.25	0.90032	0.99589	−0.912	−0.03574	0.88
0.35	0.81033	0.99196	−1.827	−0.07012	1.75
0.45	0.69865	0.98673	−3.115	−0.116	3

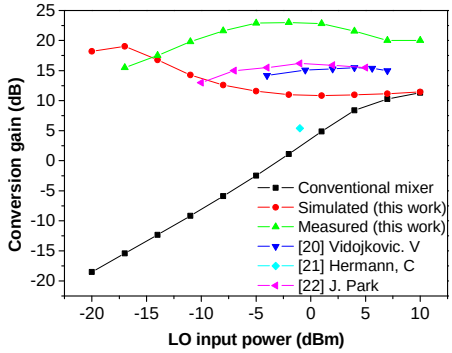

Figure 12. The conversion gain comparison between the DBGC CAAB mixer and other works.

cluded that by incorporating the current bleeding *LO* **Amp**, not only the conversion gain is enhanced, but also the *LO* power requirement is relieved by more than 20 dB. The comparison with other published works [20-22] reveals that the DBGC CAAB mixer has the highest gain but requiring the lowest *LO* power requirement.

3.6. Linearity, *LO* Power Leakage and Operation Bandwidth

The output voltage swing is examined by terminating an oscilloscope at the IF (10 MHz) port. The maximum voltage swing (peak-to-peak voltage) was measured to be 1.1 V when the RF port was fed by −11 dBm input power (see **Figure 13**).

Figure 14 shows the measured third order intermodulation (IP3) of the DBGC CAAB mixer at different *LO* power levels. When the switch pair is fed with a −5 dBm *LO* power, the IIP3 obtained is 3 dBm. When the *LO* power is −17 dBm, the mixer still has an IIP3 point of −9 dBm. In the DBGC CAAB mixer, the *LO* amplitude is amplified by five (5) times. Hence, attention is drawn to the *LO* power leakage. By examining the *LO* power at RF and IF port, it is found that the *LO* to IF port leakage is smaller than −90 dBm. The *LO* to RF power leakage is measured to be less than −60 dBm (see **Figure 15**). The good *LO*-IF isolation achieved is attributed to use of the double-balanced topology.

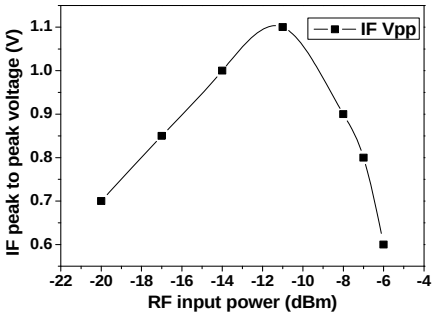

Figure 13. IF peak-to-peak voltage versus RF input power. (The result is measured with the termination of oscilloscope at IF port).

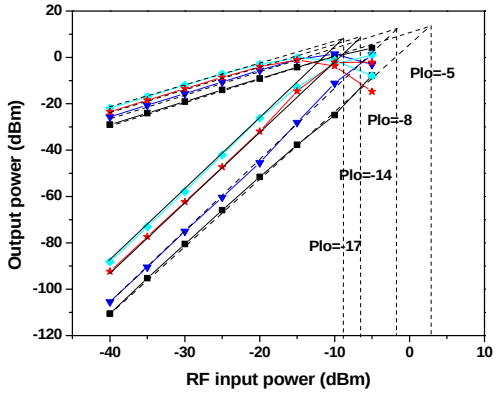

Figure 14. IIP3 of the DBGC CAAB mixer at different *LO* level.

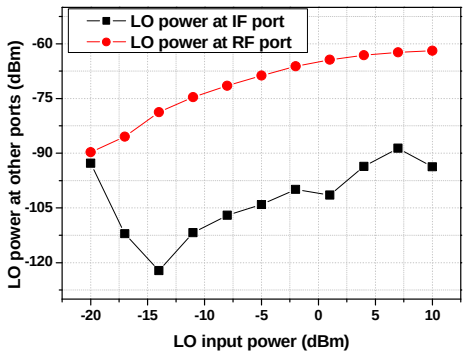

Figure 15. *LO* power leakage to RF port and IF port.

The DBGC CAAB mixer is designed for 2.4 GHz ISM band application. **Figure 16** shows the gain performance at 2.4 - 2.4835 GHz when the IF frequency is 10 MHz. In the whole band, the conversion gain of the proposed mixer varies from 19 dB to 21 dB, featuring good gain flatness.

4. Performance Summary and Comparison

Table 2 summarizes the performances of the DBGC CAAB mixer. To evaluate the mixer comprehensively, a benchmarking figure of merit, FOM, is presented:

$$FOM = 10 \cdot \log\left\{\frac{10^{(\text{Gain}-2NF+IIP3-10-P_{LO})/20} \cdot f_0/1\ \text{KHz}}{P_{DC}/1\ \text{mW}}\right\} \quad (21)$$

The *FOM* takes incorporates important parameters including Gain, *NF*, *IIP*3, *LO* power, *DC* power and operating frequency into considerations. The *FOM* values are listed in **Table 2** for comparison. From the comparison, it is found that the DBGC CAAB mixer has the lowest *LO* power requirement (−17 dBm) and the highest gain (15.7 dB), while maintaining a relatively lowest noise figure of 9.7 dB.

5. Conclusion

A current bleeding with *LO* amplification mixer based on current reuse topology is designed and implemented. The developed double balanced Gilbert-cell class-A amplifier bleeding mixer (DBGC CAAB mixer) has the highest conversion gain at the lowest *LO* power when compared to mixers formerly investigated. The DBGC CAAB mixer is implemented by using 0.18-μm CMOS technology and operates at the 2.4 GHz ISM application with 10 MHz intermediate frequency. The power consumption is 12 mA at 1.5 V supply voltage. With the novel *LO* amplification and current reuse technique, the mixer features an excellent high gain of 17.5 dB at a very low *LO* power feeding of −14 dBm. The noise performance is also good. The DBGC CAAB mixer features a noise figure of 10.7 dB, thus rendering the resulting noise to be suppressed to [8.7 dB, 12.4 dB]. In contrast, in the conventional mixer, the noise figure varies from 13 dB to 46 dB at the same *LO* feed. It is important to point out that, compared to the other mixer investigations, the DBGC CAAB mixer features the highest FOM figure within a wide range of *LO* power.

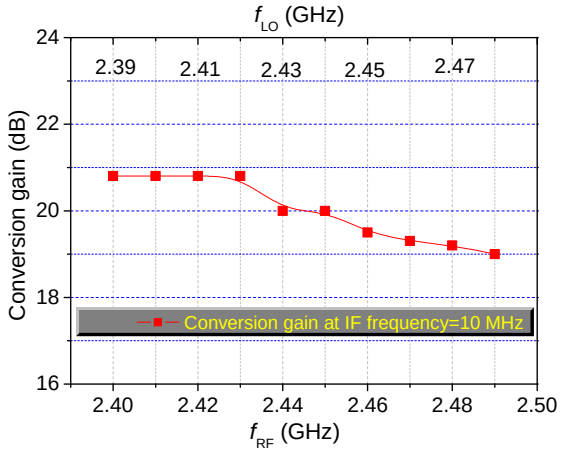

Figure 16. Conversion gain of the DBGC CAAB mixer versus frequency when IF frequency = 10 MHz.

Table 2. The performance of the DBGC CAAB mixer w.r.t. other works.

Publication	Technology	*RF*	*VDD*	P_{DC}	P_{LO}	Gain	*NF*	P_{1dB}	IIP_3	*FOM*
	CMOS	GHz	V	mW	dBm	dB	dB	dBm	dBm	dB
Darabi [5] (bleed)	0.13 μm	2	1.2	2.4	-	0.5	13.5	−1.5	10.5	-
V. Vidojkovic [20]	0.18 μm	2.4	1.8	8.1	−2	15.7	12.9	-	1	46.2
C. Hermann [21]	0.13 μm	2.5	0.6	1.6	−1	5.4	14.8	−9.2	−2.8	44
J. Park [22] (bleed)	0.18 μm	5	-	7	−1	16.2	9.8	-	−5	46.6
P. J. Sulivan [23]	0.8 μm	1.9	5	133	−3	9.7	7.8	-	−1	34.6
This work	**0.18 μm**	**2.4**	**1.5**	**18**	**−17**	**15.7**	**10.7**	**−10**	**−9**	**48.3**
This work	**0.18 μm**	**2.4**	**1.5**	**18**	**−14**	**17.5**	**10.5**	**−12**	**−8**	**48.0**
This work	**0.18 μm**	**2.4**	**1.5**	**18**	**−5**	**23**	**9.7**	**−10**	**3.5**	**47.6**

REFERENCES

[1] K. Chang, I. Bahl and V. Nair, "RF and Microwave Circuit and Component Design for Wireless Systems," Wiley-Interscience, New York, 2002.

[2] H. Darabi and A. A. Abidi, "Noise in RF CMOS Mixers: A Simple Physical Model," *IEEE Journal of Solid State Circuits*, Vol. 35, No. 1, 2000, pp. 15-25. doi:10.1109/4.818916

[3] D. Manstretta, R. Castello and F. Svelto, "Low 1/f Noise CMOS Active Mixers for Direct Conversion," *IEEE Transactions on Circuits and Systems II*, Vol. 48, 2001, pp. 846-850. doi:10.1109/82.964998

[4] H. Darabi and J. Chiu, "A Noise Cancellation Technique in Active RF-CMOS Mixers," *IEEE Journal of Solid-State Circuits*, Vol. 40, No. 12, 2005, pp. 2628-2632. doi:10.1109/JSSC.2005.857428

[5] M. T. Terrovitis and R. G. Meyer, "Noise in Current Commutating CMOS Mixers," *IEEE Journal of Solid-State Circuits*, Vol. 34, 1999, pp. 772-783. doi:10.1109/4.766811

[6] M. Krcmar, V. Subramanian, M. Jamal Deen and G. Boeck, "High Gain Low Noise Folded CMOS Mixer," *European Conference on Wireless Technology*, Amsterdam, 27-28 October 2008, pp. 13-16.

[7] V. Vidojkovic, J. Van der Tang, A. L. Leeuwenburgh and A. van Roermund, "A High Gain, Low Voltage Folded-Switching Mixer with Current-Reuse in 0.18 µm CMOS," *IEEE Digest of Papers. Radio Frequency Integrated Circuits* (*RFIC*) *Symposium*, Fort Worth, 6-8 June 2004, pp. 31-34.

[8] J. Harvey and R. Harjani, "Analysis and Design of an Integrated Quadrature Mixer with Improved Noise, Gain and Image Rejection," *The* 2001 *IEEE International Symposium on Circuits and Systems*, Vol. 4, Sydney, 6-9 May 2001, pp. 786-789.

[9] B. Gilbert, "The Micromixer: A Highly Linear Variant of the Gilbert Mixer Using a Bisymmetric Class-AB Input Stage," *IEEE Journal of Solid-State Circuits*, Vol. 32, No. 9, 1997, pp. 1412-1423. doi:10.1109/4.628753

[10] M. L. Schmatz, C. Biber and W. Baumberger, "Conversion Gain Enhancement Technique for Ultra Low Power Gilbert Cell Down Mixers," 17*th Annual IEEE Gallium Arsenide Integrated Circuit* (*GaAs IC*) *Symposium*, San Diego, 29 October-1 November 1995, pp. 245-248.

[11] G. Z. Fatin, M. S. Oskooei and Z. D. K. Kanani, "A Technique to Improve Noise Figure and Conversion Gain of CMOS Mixers," 50*th Midwest Symposium on Circuits and Systems*, Montreal, 5-8 August 2007, pp. 437-440.

[12] J. Yoon, H. Kim, C. Park, J. Yang, H. Song, S. Lee and B. Kim, "A New RF CMOS Gilbert Mixer with Improved Noise Figure and Linearity," *IEEE Transactions on Microwave Theory and Techniques*, Vol. 56, No. 3, 2008, pp. 626-631.

[13] J. Lerdworatawee and W. Namgoong, "Generalized Linear Periodic Time-Varying Analysis for Noise Reduction in an Active Mixer," *IEEE Journal of Solid-State Circuits*, Vol. 42, No. 6, 2007, pp. 1339-135.

[14] T. Melly, A.-S. Porret, C. C. Enz and E. A. Vittoz, "An Analysis of Flicker Noise Rejection in Low-Power and Low-Voltage CMOS Mixers," *IEEE Journal of Solid-State Circuits*, Vol. 36, No. 1, 2001, pp. 102-109.

[15] L. A. MacEachern and T. Manku, "A Charge-Injection Method for Gilbert cell Biasing," *IEEE Canidian Conference on Electrical and Computer Engingeering*, Waterloo, 24-28 May 1998, pp. 365-368.

[16] S. G. Lee and J. K. Choi, "Current-Reuse Bleeding Mixer," *Electronics Letters*, Vol. 36, No. 8, 2000, pp. 696-697. doi:10.1049/el:20000556

[17] K. Xuan, K. F. Tsang, S. C. Lee and W. C. Lee, "High-Performance Current Bleeding CMOS Mixer," *Electronics Letters*, Vol. 45, No. 19, 2009, pp. 979-981.

[18] B. Razavi, "Design of Analog CMOS Integrated Circuits," McGraw-Hill, New York, 2001.

[19] D. K. Shaeffer and T. H. Lee, "A 1.5-V, 1.5-GHz CMOS Low Noise Amplifier," *IEEE Journal of Solid-State Circuits*, Vol. 32, No. 5, 1997, pp. 745-759. doi:10.1109/4.568846

[20] V. Vidojkovic, J. Van der Tang, A. Leeuwenburgh and A. H. M. Van Roermund, "A Low-Voltage Folded-Switching Mixer in 0.18-µm CMOS," *IEEE Journal of Solid-State Circuits*, Vol. 40, No. 6, 2005, pp. 1259-1264.

[21] C. Hermann, M. Tiebout and H. Klar, "A 0.6-V 1.6-mW Transformer-Based 2.5-GHz Down Conversion Mixer with +5.4-dB Gain and −2.8-dBm IIP3 in 0.13-µm CMOS," *IEEE Transactions on Microwave Theory and Techniques*, Vol. 53, No. 2, 2005, pp. 488-495.

[22] J. Park, C.-HO Lee, B.-S. Kim, and J. Laskar, "Design and Analysis of Low Flicker-Noise CMOS Mixers for Direct-Conversion Receivers," *IEEE Transactions on Microwave Theory and Techniques*, Vol. 54, No. 12, 2006, pp. 4372-4380.

[23] P. J. Sulivan, B. A. Xavier and W. H. Ku, "Low Voltage Performance of a Microwave CMOS Gilbert Cell Mixer," *IEEE Journal of Solid-State Circuits*, Vol. 32, No. 7, 1997, pp. 1151-1155.

